Climate Dynamics (2004) 22: 839–855
DOI 10.1007/s00382-004-0420-2

A. Giannini · R. Saravanan · P. Chang

The preconditioning role of Tropical Atlantic Variability in the development of the ENSO teleconnection: implications for the prediction of Nordeste rainfall

Received: 28 October 2003 / Accepted: 19 February 2004 / Published online: 12 May 2004

Abstract A comparison of rainfall variability in the semi-arid Brazilian Nordeste in observations and in two sets of model simulations leads to the conclusion that the evolving interaction between Tropical Atlantic Variability (TAV) and the El Niño-Southern Oscillation (ENSO) phenomenon can explain two puzzling features of ENSO's impact on the Nordeste: (1) the event-to-event unpredictability of ENSO's impact; (2) the greater impact of cold rather than warm ENSO events during the past 50 years. The explanation is in the 'preconditioning' role of Tropical Atlantic Variability. When, in seasons prior to the mature phase of ENSO, the tropical Atlantic happens to be evolving consistently with the development expected of the ENSO teleconnection, ENSO and TAV add up to force large anomalies in Nordeste rainfall. When it happens to be evolving in opposition to the canonical development of ENSO, then the net outcome is less obvious, but also less anomalous. The more frequent occurrence of tropical Atlantic conditions consistent with those that develop during a cold ENSO event, i.e. of a negative meridional sea surface temperature gradient, explains the weaker warm ENSO and stronger cold ENSO anomalies in Nordeste rainfall of the latter part of the twentieth century. Close monitoring of the evolution of the tropical Atlantic in seasons prior to the mature phase of ENSO should lead to an enhanced forecast potential.

A. Giannini (✉) · R. Saravanan
National Center for Atmospheric Research, Boulder, CO, USA
E-mail: alesall@iri.columbia.edu

P. Chang
Department of Oceanography, Texas A and M University, College Station, TX, USA

Present address: A. Giannini
International Research Institute for Climate Prediction, P.O. Box 1000, Palisades, NY 10964-8000, USA

1 Introduction

The interannual variability of rainfall in the semi-arid northeastern region of Brazil, or Nordeste (see Sect. 2 for a precise geographical definition), is dominated by sea surface temperature (SST) variability, of local (Atlantic) and remote (Pacific) origin (Hastenrath and Heller 1977; Moura and Shukla 1981; Ropelewski and Halpert 1987, 1996; Kiladis and Diaz 1989; Servain 1991; Hastenrath and Greischar 1993; Nobre and Shukla 1996; Uvo et al. 1998; Wallace et al. 1998; Saravanan and Chang 2000; Chiang et al. 2000, 2002; Pezzi and Cavalcanti 2001). The relationship between Nordeste rainfall and tropical SST manifests itself in the fidelity with which simulations obtained by forcing atmospheric general circulation models (AGCMs) with the historical record of SST reproduce the observed interannual variability of Nordeste rainfall (Palmer et al. 1992; Harzallah et al. 1996; Sperber and Palmer 1996; Moron et al. 1998; Koster et al. 2000; Saravanan and Chang 2000).

In this study we use one such model, CCM3, version 3 of the Community Climate Model developed at the National Center for Atmospheric Research (NCAR), and validate its simulation of Nordeste variability against observations. When CCM3 is forced by specifying observed SSTs between 1950 and 1994, it reproduces the observed variability of Nordeste rainfall with a high degree of accuracy. In Fig. 1 we compare indices of Nordeste rainfall variability in the model and in observations, taken from the Global Historical Climate Network (GHCN) of stations. (Observed data and model output used in this study are described in greater detail in Sect. 2). The indices in Fig. 1a, of rainfall averaged over austral fall (March, April and May, or MAM), the local rainy season, correlate at a value of 0.83. Figure 1b and c depict the correlation patterns of the same observed and modeled indices respectively with simultaneous SST. High values span the tropical oceans. They

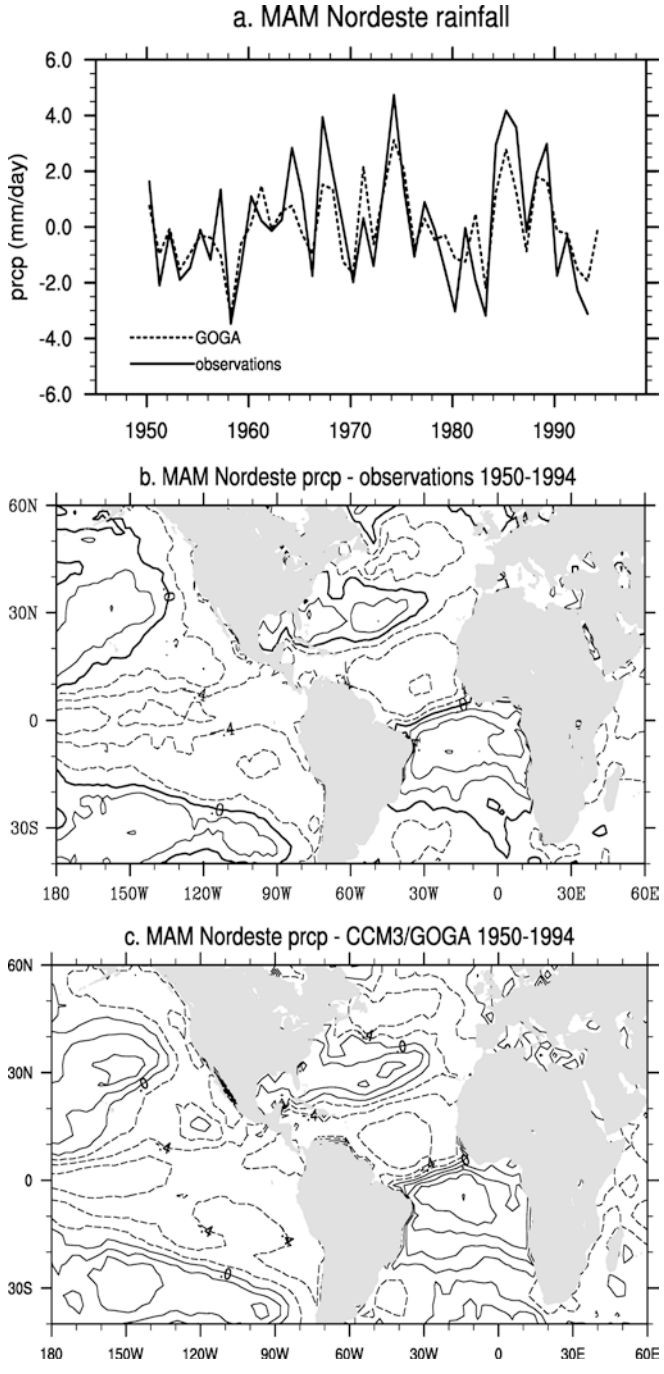

Fig. 1 General features of the simulation of Nordeste rainfall variability with CCM3. **a**: comparison of observed (*solid line*) and CCM3-GOGA (*dashed line*) time series of rainy season (March–May) precipitation. (For a definition of Nordeste, see Sect. 2). The modeled time series is the ensemble average of five integrations. **b**, **c**: Simultaneous correlation maps of the observed and modeled (GOGA) regional rainfall indices with SST. Contour interval is every 0.2 and negative values are *dashed*

are of the same, negative sign in the tropical Pacific and tropical North Atlantic, of opposite, positive sign in the tropical South Atlantic.

The widely accepted interpretation of the correlation pattern in Fig. 1 (e.g., Hastenrath 1991) is that the dominant forcing driving Nordeste rainfall variability is local to the tropical Atlantic, with the remote influence of the tropical Pacific playing a secondary role, at times reinforcing, at times weakening the local coupling (Uvo et al. 1998; Pezzi and Cavalcanti 2001). Many studies since the seminal works of Hastenrath and Heller (1977) and Moura and Shukla (1981) have described and modeled the association between Atlantic SST and the meridional displacement of the Atlantic Intertropical Convergence Zone (ITCZ). The dominant pattern of Tropical Atlantic Variability (TAV) is one characterized by coherent, zonally-symmetric anomalies in SST, surface winds and net surface heat flux, organized along the meridional direction (Nobre and Shukla 1996; Seager et al. 2001). This coupled SST/wind/evaporation pattern has the potential to reinforce itself through a thermodynamic feedback (Chang et al. 1997; Xie 1999): a warm SST anomaly on either side of the thermal equator decelerates the trade winds in the hemisphere (Lindzen and Nigam 1987) local to the SST anomaly, and accelerates them in the remote hemisphere. The component of evaporation that is directly proportional to wind speed is weaker than average in the local hemisphere, stronger than average in the remote hemisphere, resulting in a positive feedback on the initial SST anomaly. SST anomalies would grow indefinitely if it were not for the natural tendency of the ocean-atmosphere system to restore to equilibrium by damping air-sea temperature differences through increased net surface heat flux. Ocean dynamics can also contribute to damping SST anomalies, e.g., by means of the meridional ocean heat transport associated with anomalous temperature gradients (Chang et al. 1997; Kushnir et al. 2002).

By influencing the meridional SST gradient, TAV affects the meridional location of the ITCZ, the dominant rain-bearing system for the northern Northeast Brazil region focus of this study (Hastenrath and Heller 1977; Moura and Shukla 1981; Nobre and Shukla 1996). The presence of a positive SST anomaly in the north tropical Atlantic, hence of an anomalously positive, or northward SST gradient in March-May can hinder the seasonal excursion of the Atlantic ITCZ into the Southern Hemisphere, causing drought in the Nordeste. Conversely, the presence of a positive SST anomaly in the south tropical Atlantic, hence of an anomalously negative, or southward SST gradient, attracts the ITCZ southward, favoring in extreme cases a greater probability for the recurrence of heavy rains and floods. (The opposite of what described here is true of negative SST anomalies in either hemisphere.)

The subordinate nature of the role played by ENSO is inferred from the significant, but weak statistical relationship between Nordeste rainfall and Niño-3, a commonly used indicator of ENSO defined as the SST anomaly in the central and eastern equatorial Pacific, between 5°S and 5°N, 150°W and 90°W. This correlation is of the order of –0.4 over the 100 years or so of

instrumental record, considerably weaker than the correlation of Nordeste rainfall with the measure of TAV chosen in this work, i.e., the difference in SST between the northern and southern tropical Atlantic, which is of the order of –0.6 over 1950–1994 (also see Sect. 3). This interpretation is certainly justifiable in dynamical terms also. Due to the phase-locking of ENSO to the seasonal cycle, an ENSO event is typically not at its strongest during the Nordeste rainy season, but either in its onset or decay phase. In this case, either the atmospheric teleconnection has not had time to fully develop, or it has already considerably weakened. In prediction experiments with an atmospheric model coupled to a mixed-layer ocean, overall comparable results are obtained in the prediction of March–May Nordeste rainfall when global or Atlantic only SSTs observed in December are imposed as initial conditions (Chang et al. 2003).

However, it is well known that climate variability local to the tropical Atlantic, most notably in the tropical North Atlantic basin, is not independent of the tropical Pacific. ENSO affects the tropical Atlantic climate directly, through atmospheric anomalies, and indirectly, through the effect the latter have on SST. ENSO-related atmospheric anomalies are responsible for changes in the speed of the tropical North Atlantic trade winds, changes which peak during the mature phase of ENSO, i.e. towards the end of the calendar year. These wind speed anomalies in turn drive net surface heat flux anomalies (Cayan 1992; Seager et al. 2000) which result in a local SST response peaking in Southern Hemisphere fall (Curtis and Hastenrath 1995; Enfield and Mayer 1997; Giannini et al. 2000; Czaja et al. 2002), i.e. with a delay of about one season with respect to mature ENSO conditions.

The direct effect of ENSO-related atmospheric anomalies on tropical Atlantic climate, and on Northeast Brazil rainfall was shown to be significant by Saravanan and Chang (2000) and Giannini et al. (2001b). In comparing the same ensemble of integrations with CCM3 used here, i.e. the ensemble forced with global, observed SST (GOGA, or Global Ocean Global Atmosphere), to an ensemble where SST was prescribed as observed in the tropical Atlantic only (18°S to 18°N; TAGA, or Tropical Atlantic Global Atmosphere), they found that in the latter the relationship between Nordeste rainfall and tropical North Atlantic SSTs was considerably weaker than in the former. In GOGA this relationship compounds the direct and indirect effects of ENSO, i.e. the effect of ENSO-related atmospheric anomalies and of remotely-forced SST anomalies on Nordeste rainfall. In TAGA only the latter is present, hence the response is weaker.

Given the interconnectedness of ENSO and TAV, in this study we jointly consider the impacts of ENSO and TAV on Nordeste rainfall, and choose to frame the ENSO/TAV/Nordeste rainfall interaction as a modulation by TAV of the impact of ENSO on Nordeste rainfall. We will show that the tropical South Atlantic is as important, in exciting TAV, as its more studied and better understood tropical North Atlantic counterpart, and that the competition between northern and southern tropics mediated by TAV is crucial to the explanation of the relatively low correlation between ENSO and Nordeste rainfall, and to the prediction of Nordeste rainfall. The superposition of two weakly interacting impacts, i.e. those of ENSO and TAV on Nordeste, can also explain the weaker relationship between warm ENSOs and Nordeste rainfall, compared to the stronger relationship in cold ENSOs. In the last 50 years or so, a tropical Atlantic preconditioned to favor the canonical development of the ENSO teleconnection has occurred more frequently in cold rather than in warm ENSO events. This conjuncture has resulted in the effective superposition of the impacts of ENSO and TAV, hence of significant Nordeste rainfall anomalies, in cold more frequently than in warm ENSO events. This occurrence may be related to the recent positive trend in the North Atlantic Oscillation (Giannini et al. 2001a), and associated cooling of the tropical North Atlantic.

Section 2 contains a description of the data used, observations and model experiments. Sect. 3 lays out the observational background to justify the focus on ENSO years. In Sect. 4 results are presented from a diagnostic study of Nordeste rainfall variability in observations and in the ensemble of integrations forced with globally observed SSTs. Model integrations forced with observed tropical Pacific SSTs only, and their potential for dynamical seasonal prediction, are the subject of Sect. 5. Section 6 contains a discussion and concluding remarks.

2 Data and methods

The analysis of observed variability of Nordeste rainfall hinges on station data extracted from the Global Historical Climate Network (GHCN) archive, maintained at the National Oceanic and Atmospheric Administration (NOAA) National Climatic Data Center (NCDC) (Vose et al. 1992; Peterson et al. 1994; Easterling et al. 1996; see the NOAA/NCDC website at http://lwf.ncdc.noaa.gov/oa/ncdc.html . Also available from the Data Library maintained by the International Research Institute for Climate Prediction, Columbia University (IRI; http://iridl.ldeo.columbia.edu/ .)) Nordeste rainfall is represented by 13 stations in the Brazilian states of Ceará, Pernambuco, Piaui and Rio Grande do Norte, all within 10°S of the equator. This region should more appropriately be referred to as the northern Nordeste (Magalhaes 1993; Nobre and Shukla 1996). It is that portion of northeastern Brazil which by virtue of its proximity to the equator is exclusively affected by tropical weather systems associated with the ITCZ. The 13 stations were extracted from GHCN in view of the completeness of their records during the local rainy season, i.e. austral fall (March to May, or MAM). The geographical limits of the Nordeste in the analysis of model output, 10°S to 0°N, and 45°W to 15°W, were chosen based on spatial coherence in a principal

component analysis of the seasonal cycle of rainfall (not shown). This choice is justified *a posteriori* by the spatial coherence of ENSO-related rainfall anomalies, which cover the Nordeste and adjacent western equatorial Atlantic (see Fig. 6).

Model validation makes use of two five-member ensembles of multi-decadal integrations carried out with the same state-of-the-art atmospheric model, CCM3, the spectral model developed at NCAR (see Kiehl et al. 1998 and companion papers in the same issue of *J. Climate*). CCM3 is integrated during 1950–1994 at its standard resolution, triangular truncation at wave number 42 in the horizontal and 19 vertical levels, using two configurations of boundary conditions, abbreviated as GOGA and POGAML. GOGA, or Global Atmosphere Global Ocean, is integrated imposing the history of global, observed SSTs as the oceanic boundary condition. POGAML, or Pacific Ocean Global Atmosphere-Mixed Layer, is integrated specifying observed SSTs in the tropical Pacific basin only. Outside of the tropical Pacific, SST (T in the model equation later) is computed based on simulated ocean-atmosphere heat fluxes, corrected for the absence of ocean dynamics using a 'q-flux' formulation:

$$\rho Ch\frac{\partial T}{\partial t} = F + Q$$

where ρ and C are density and specific heat of the ocean (1000 kgm^{-3}and 1810 Jkg^{-1} K^{-1}respectively), h is mixed layer depth, fixed at the annual mean value computed from observations (Levitus and Boyer 1994), and F is the prognosed net atmosphere-to-ocean heat flux. Q is a correction term responsible for maintaining the observed seasonal cycle of SST in the absence of ocean dynamics in the model. For each month m:

$$Q^m = \rho Ch^m\frac{T^{m+1} - T^{m-1}}{d^{m+1} - d^{m-1}} - F^m$$

where h^m and T^m are the climatological mixed layer depth and temperature for month m, and d^m is the mid-month calendar day (Kiehl et al. 1996).

The POGAML setup is equivalent to the TOGA-ML (Tropical Ocean Global Atmosphere-Mixed Layer) set-up widely applied to explore the impact of the ENSO teleconnection, or 'atmospheric bridge', to the extra-tropical atmosphere-ocean system and feedbacks (Lau and Nath 1994, 1996; Lau 1997; Alexander et al. 2002). This configuration is of particular relevance to the dynamical seasonal prediction problem in the Nordeste. It captures the nature of ENSO and TAV, characterizing ENSO as a remote forcing, and interannual TAV as a local thermodynamic, ocean-atmosphere interaction (Chang et al. 1997; Seager et al. 2001; Biasutti 2000), thus allowing the study of the predictability that comes from the interaction between tropical Pacific and tropical Atlantic climate variability.

In the Introduction, output from a third five-member ensemble of integrations with CCM3 was also briefly discussed. This ensemble was referred to as TAGA (Tropical Atlantic Global Atmosphere) and was conceived by Saravanan and Chang (2000) specifically to separate the effect of Atlantic SSTs on Tropical Atlantic Variability from the remote atmospheric influence of ENSO on TAV. As mentioned in the Introduction, in TAGA CCM3 was forced with observed SST in the tropical Atlantic basin only (18°S to 18°N), and monthly varying climatological SSTs elsewhere.

In the following, statistics from observations and from the ensemble averages of CCM3-GOGA and CCM3-POGAML are compared over the common period, 1950–1994. ENSO events are selected based on the observed Niño-3 index of Kaplan et al. (1998), which blends the Kaplan et al. (1998) Reduced Space Optimal Analysis SST product, used until October 1981, with Reynolds and Smith (1994) SSTs, used from November 1981 to present. A December-January Niño-3 greater than 1 °C or less than –0.75 °C identifies the years ending in December and starting in January as year(0) and year(1) of a warm or cold ENSO event respectively (Rasmusson and Carpenter 1982). (The asymmetry in the threshold chosen for warm and cold ENSO events parallels the skewness in the distribution of Niño-3 toward warm values.) Year(0) is the year of onset and growth, year(1) the year of decay. Remaining years are classified as neutral. During 1950–94 there were nine warm ENSO events (1957–58, 1965–66, 1969–70, 1972–73, 1976–77, 1982–83, 1986–87, 1987–88 and 1991–92), and eight cold ENSO events (1955–56, 1964–65, 1967–68, 1970–71, 1973–74, 1975–76, 1984–85 and 1988–89).

Tropical Atlantic Variability is characterized by the strength of the inter-hemispheric gradient in SST - the difference between the averages of SST in the tropical North Atlantic (tNA, defined as the average between 5°N and 25°N, 60°W and 30°W) and in the tropical South Atlantic (tSA, defined as the average between 25°S and 5°S, 30°W and 0°E). Because we are interested in the 'preconditioning role' of TAV in the development of the ENSO teleconnection to the tropical Atlantic, in Sects. 4 and 5 we select years based on the gradient index in December–February of year(1) of ENSO (DJF(1)), i.e. during the season preceding the development of the strongest ENSO- and TAV-related responses in the tropical Atlantic. Nordeste rainfall anomalies are consistently computed over the local rainy season, i.e. March–May, of year(1), the year following mature ENSO conditions (MAM(1)).

3 ENSO's role in TAV: the Nordeste rainfall-tropical Atlantic SST relation revisited

We start with a re-assessment of the Nordeste rainfall-tropical Atlantic SST relationship in observations, which lays out the groundwork to justify our focus on ENSO years. As discussed in the Introduction, the relationship depicted in Fig. 1 is most often portrayed

as the sum of the dominant local and recessive remote SST impacts. In fact, assuming that tropical Atlantic SST variability is predominantly local can be misleading, given ENSO's role in TAV (Curtis and Hastenrath 1995; Nobre and Shukla 1996; Saravanan and Chang 2000). In Fig. 2 we present evidence to support an alternative framework, i.e. that ENSO and TAV play equally important roles in Nordeste rainfall variability, and that from their combination can arise extremely anomalous Nordeste rainfall years (Hastenrath and Heller 1977; Uvo et al. 1998; Pezzi and Cavalcanti 2001). In the scatterplot of a Nordeste rainfall index, along the ordinate axis, versus an index of the Atlantic SST gradient, along the abscissa (Fig. 2a), ENSO years are represented by solid circles, non-ENSO, or neutral years by open squares. The contribution from ENSO years is fundamental in imprinting a negative slope to the regression. This situation is reflected in the simultaneous (March–May) correlation values of Nordeste rainfall with the Atlantic SST gradient index, which is –0.64 over all years between 1950 and 1994, rises to –0.84 when ENSO years only are taken into account, and plummets to –0.37 in neutral years. To verify that the differences among these correlation values are not the consequence of undersampling, we use a Monte-Carlo simulation. We randomly pick 1000 times a number of years equal to the smaller number of ENSO years (17 events) from the observed larger number of non-ENSO years (27 years, to avoid counting the decaying phase of the 1949–1950 cold ENSO). A correlation value equal to or greater than that obtained for ENSO years (–0.84) is repeated in non-ENSO years with a frequency smaller than 1%.

When ENSO and TAV are 'in phase', the direct or atmospheric component of the ENSO teleconnection adds to the local forcing of TAV to give consistently larger anomalies, in Atlantic SST and in Nordeste rainfall. When TAV is left alone to force Nordeste rainfall through the meridional SST gradient, rainfall anomalies are, on average, weaker and less consistent, possibly because the forcing SST anomalies themselves are weaker. Variability in the Atlantic SST gradient is higher in ENSO than in non-ENSO years. Standard deviations of the MAM Atlantic SST gradient index are respectively 0.66 °C and 0.4 °C in ENSO and neutral years, significantly different at the 95% level according to an *F*-test (Fisher 1970).

ENSO can reinforce TAV and its influence on Nordeste rainfall. When maps of the Nordeste rainfall-SST correlation are computed separately on ENSO and non-ENSO years, in Fig. 2b,c, and compared to the map computed on all years, in Fig. 1b, the spatial patterns are similar, but the amplitude in ENSO years is much stronger than in non-ENSO years. To conclude, a large portion of Nordeste rainfall variability related to the Atlantic meridional SST gradient is a consequence of the ENSO-TAV interaction. Because the Nordeste-SST relationship is stronger in ENSO than in non-ENSO years, in keeping with our goal of quantifying potential predictability of Nordeste rainfall, in the remainder of this study we will focus on ENSO years.

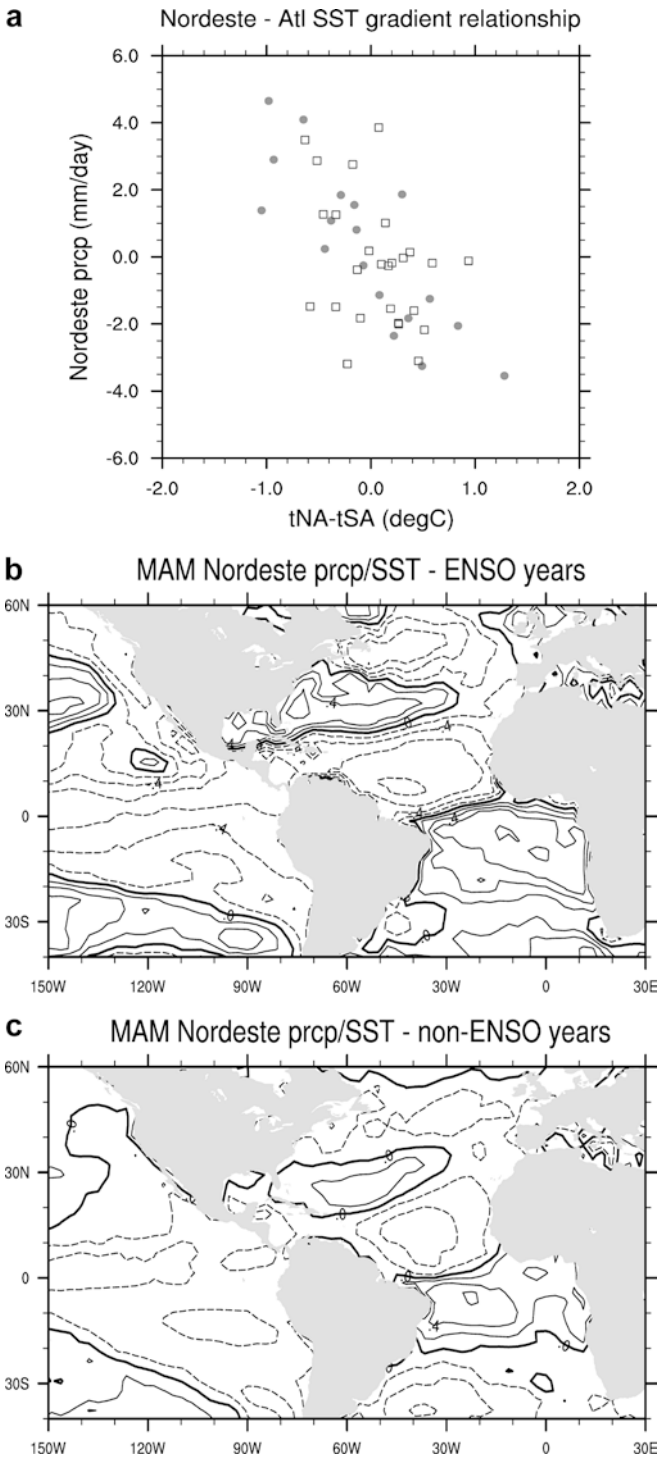

Fig. 2 Comparison of the Nordeste rainfall-Atlantic SST relationship in ENSO and non-ENSO years. **a**: scatterplot of observed Nordeste anomalies versus the observed Atlantic SST gradient. *Solid circles* denote ENSO years, *open squares* non-ENSO years. **b**, **c**: Simultaneous correlation maps of observed Nordeste rainfall with SST in MAM(1) of ENSO and non-ENSO years. Contour interval is every 0.2 and negative values are *dashed*

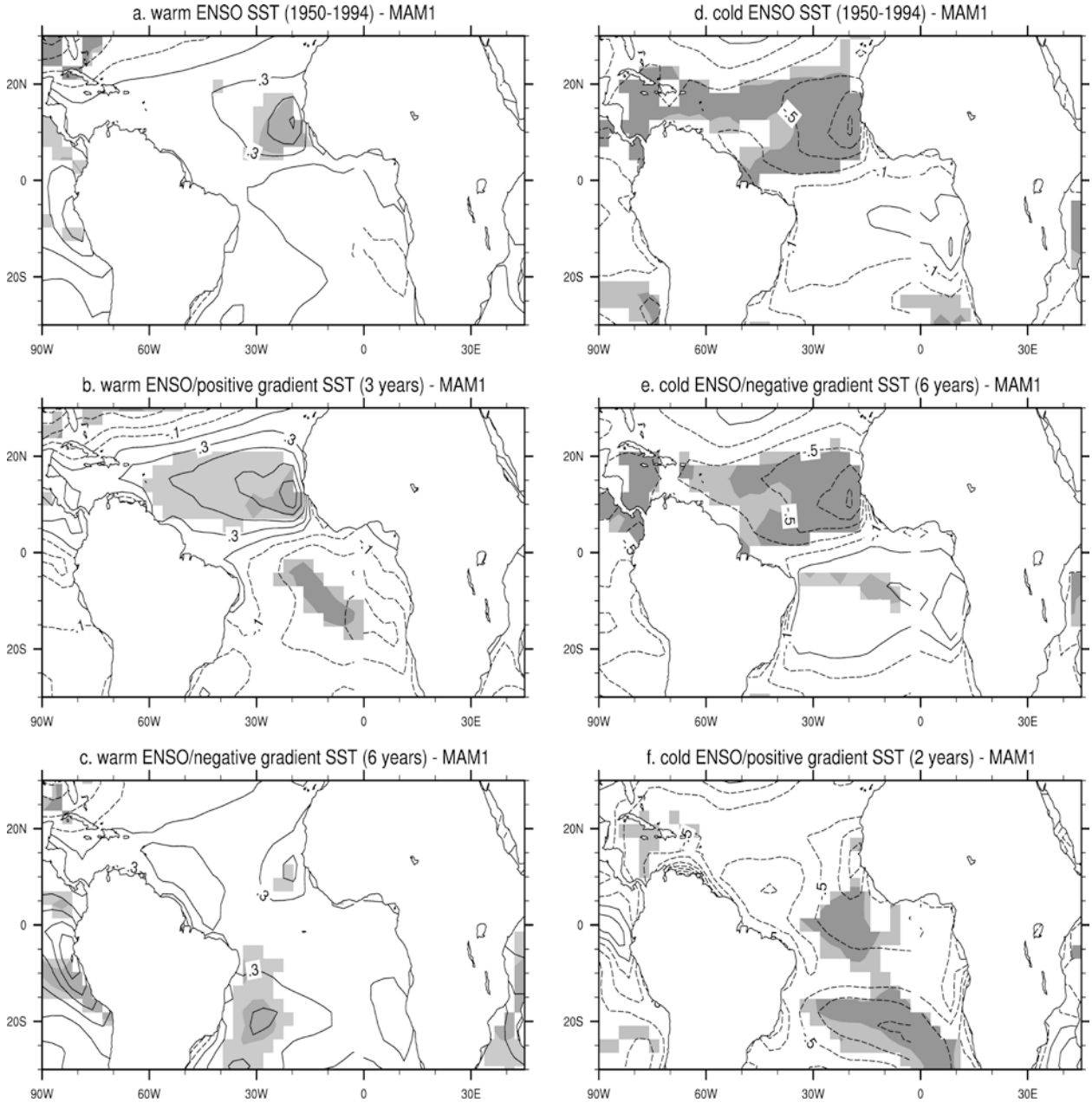

Fig. 3 Warm ENSO-minus-neutral (*left column*) and cold ENSO-minus-neutral (*right column*) composites of SST in MAM(1). Contour interval is every 0.2 °C starting from 0.1 °C, negative values are *dashed*, and *light*/*dark shading* indicates statistical significance at the 95/99% level. *Top panels*: the average of all ENSO years: 1957–58, 1965–66, 1969–70, 1972–73, 1976–77, 1982–83, 1986–87, 1987–88 and 1991–92 were warm ENSO events, 1955–56, 1964–65, 1967–68, 1970–71, 1973–74, 1975–76, 1984–85 and 1988–89 were cold ENSO events. *Middle panels*: concordant ENSO/gradient years 1958, 1966 and 1970 make up the warm ENSO/positive gradient composite, 1965, 1968, 1971, 1974, 1985 and 1989 the cold ENSO/negative gradient composite. *Bottom panels*: discordant ENSO/gradient years 1973, 1977, 1983, 1987, 1988 and 1992 make up the warm ENSO/negative gradient composite, 1956 and 1976 the cold ENSO/positive gradient composite

4 The preconditioning role of TAV in the development of the ENSO teleconnection to the tropical Atlantic

If ENSO is instrumental in TAV, then why is the ENSO-Nordeste rainfall relationship weak?

In the following we show that the successful superposition of ENSO and TAV effects is not a random occurrence, but depends on the preconditioning of TAV on the development of the ENSO teleconnection to the tropical Atlantic.

4.1 Tropical Atlantic SST variability: interaction of remote and local effects

To diagnose the interaction of Pacific and Atlantic forcings we assume for a moment that ENSO and TAV

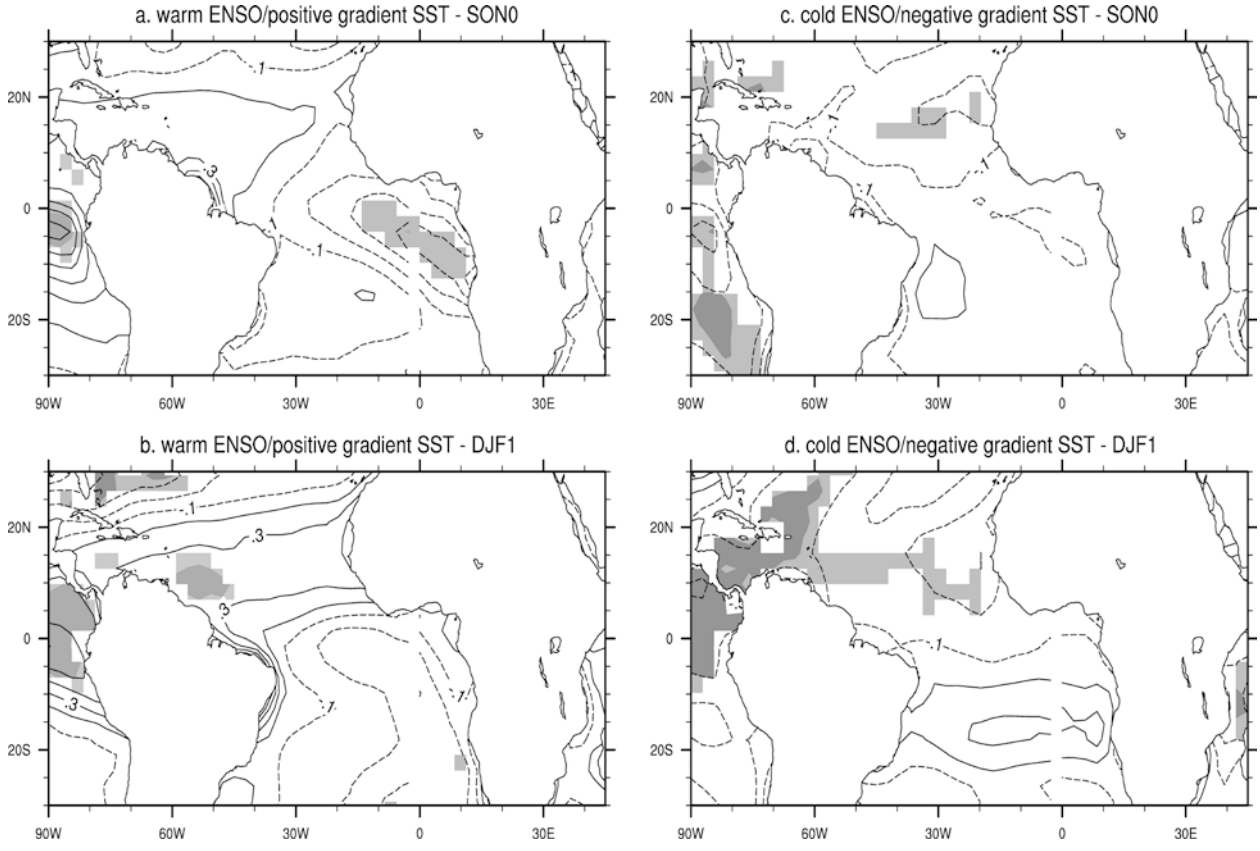

Fig. 4 The evolution of SST anomalies in concordant years (warm ENSO/positive gradient, *left column*; and cold ENSO/negative gradient, *right column*) from September–November of year(0) to March–May of year(1). Contour interval is every 0.2 °C starting at 0.1 °C, and *light*/*dark shading* represents the 95/99% level of statistical significance

are independent. We analyze Atlantic SST anomalies in warm and cold ENSO years, further stratifying according to the sign of the DJF(1) Atlantic SST gradient, defined in Sect. 2, hereafter referred to as the 'gradient'.

Statistical significance of the difference of the means is assessed by applying a two-tailed Student *t*-test (von Storch and Zwiers 1999). Given two sub-populations x and y, made up of n_x and n_y samples each, the parameter t is defined by:

$$t = \frac{\bar{x} - \bar{y}}{\sigma_{pooled}}$$

where $\sigma^2_{pooled} = \frac{n_x\sigma_x^2 + n_y\sigma_y^2}{n_x + n_{y-2}} \left(\frac{1}{n_x} + \frac{1}{n_y}\right)$ is the pooled variance. The significance of t is evaluated based on the total number of degrees of freedom, $n_x + n_y - 2$. The lighter and darker shadings in Figs. 3–10 represent the 95% and 99% significance levels respectively.

Figure 3 depicts composite maps of warm ENSO-minus-neutral and cold ENSO-minus-neutral differences in SST averaged over March–May of year(1) (MAM(1)) of ENSO. In the top panels of Fig. 3 note that: (1) tropical North Atlantic SST anomalies are larger and statistically more significant in cold ENSO than in warm ENSO events; (2) in warm ENSO events there is a hint of anomalously warm tropical South Atlantic SSTs, off the coast of South America, i.e. of anomalies of the same sign as those expected from ENSO in the tropical North Atlantic. The composites in the middle panels of Fig. 3 are labelled 'concordant': ENSO and the gradient taken independently are expected to force north tropical Atlantic SST anomalies of the same sign, and their combination can give rise to extreme Nordeste rainfall anomalies. A warm ENSO and a positive, or northward gradient should combine to give negative Nordeste rainfall anomalies. A cold ENSO and a negative, or southward gradient should combine to give positive Nordeste rainfall anomalies. The average of March–May of 1958, 1966 and 1970 makes up the warm ENSO/positive gradient composite, the average of MAM of 1965, 1968, 1971, 1974, 1985 and 1989 the cold ENSO/negative gradient composite. The ENSO years in the bottom panels of Fig. 3 are labelled 'discordant'. ENSO and gradient taken independently would force Nordeste rainfall anomalies of opposite sign, e.g., a warm ENSO combined with a negative gradient (as in MAM of 1973, 1977, 1983, 1987, 1988 and 1992), or a cold ENSO combined with a positive gradient (as in MAM of 1956 and 1976), so that their superposition, as will be shown in the next subsection, results in incoherent, not statistically significant, by and large 'unpredictable' rainfall anomalies.

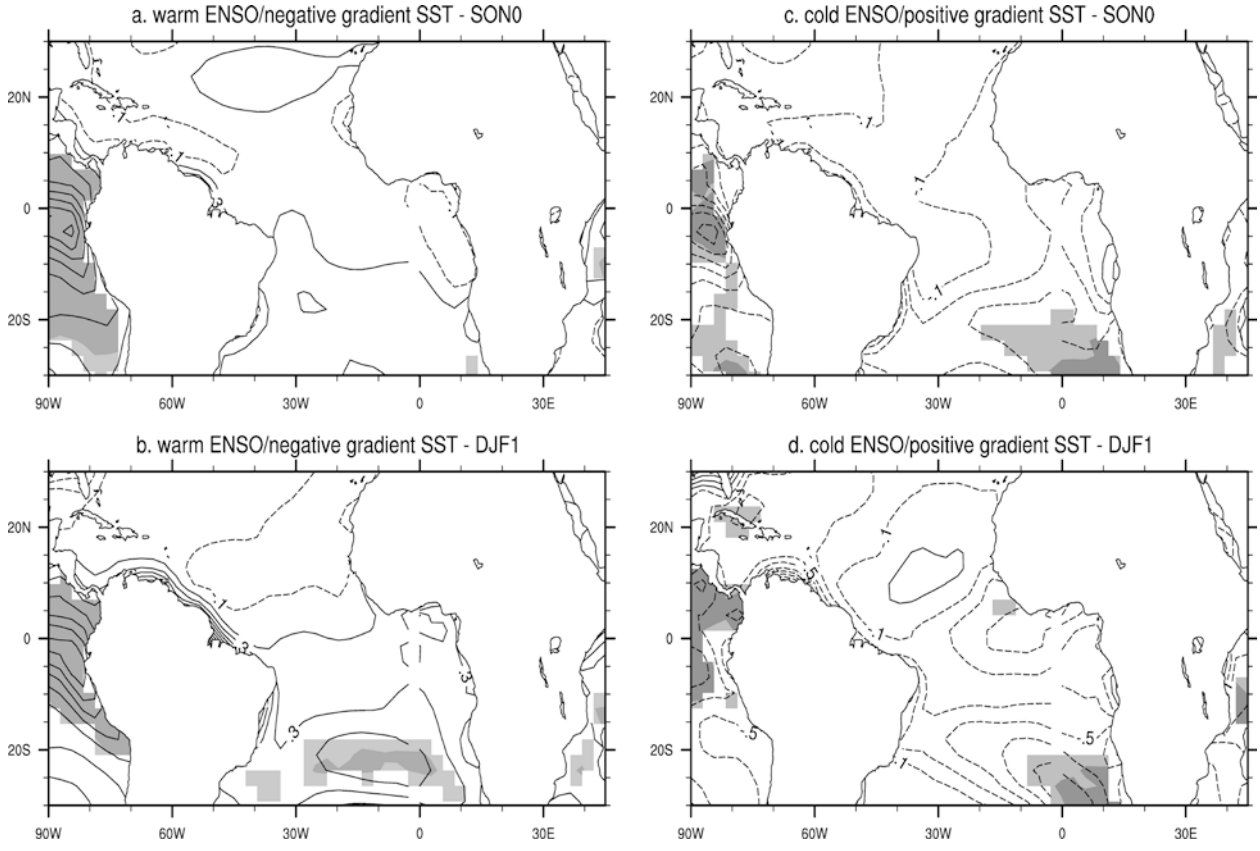

Fig. 5 The evolution of SST anomalies in discordant years (warm ENSO/negative gradient, *left column*; and cold ENSO/positive gradient, *right column*) from September–November of year(0) to March–May of year(1). Contour interval is every 0.2 °C starting at 0.1 °C, and *light*/*dark shading* represents the 95/99% statistical significance level

Table 1 Observed Nordeste rainfall anomalies (in mm/day), and *t*-values (in parentheses) in ENSO events, 1950–1994

	Warm ENSO (mm/day)	Cold ENSO (mm/day)
All ENSO years	–0.8	**+1.7**
Concordant ENSO/gradient	**–2.3** (t = 2.02)	**+2.7** (t = 3.1)
Discordant ENSO/gradient	–0.1	–1.0

Values in bold font highlight departures from the average of non-ENSO, or neutral years that are statistically significant at the 95% level

The averages of all warm and all cold ENSO events (top panels of Fig. 3) do not depict the average situation. Rather, concordant (middle panels of Fig. 3) and discordant (bottom panels of Fig. 3) composites represent mutually exclusive conditions: tropical North Atlantic SST anomalies prevail in concordant composites, as would be expected from the evolution of the 'canonical ENSO teleconnection' to the tropical Atlantic (Curtis and Hastenrath 1995; Enfield and Mayer 1997), while tropical South Atlantic anomalies, centered around 20°S, prevail in discordant SST composites. This behavior hints at two fundamentally distinct developments of tropical Atlantic SSTs in concordant and discordant ENSO years, developments in which the interaction between the tropical ENSO atmospheric bridge and Tropical Atlantic Variability plays a role.

To verify to what extent pre-existing conditions in the tropical Atlantic may influence the development of ENSO-related SST anomalies, and ultimately the predictability of Nordeste precipitation, the ENSO lifecycle in Atlantic SSTs is analyzed for concordant and discordant cases separately going back to austral spring (September–November) of year (0) (SON(0)) and summer (December–February) of year (1) (DJF(1)) (Figs. 4 and 5). Though not as statistically significant as in MAM(1), anomalies in SON(0) and DJF(1) bear many similarities to the patterns of Fig. 3. In concordant years (Fig. 4) the expected, from ENSO, sign of the Atlantic gradient is already present in SON(0) and strengthens in DJF(1). In discordant years (Fig. 5), the basin-wide meridional gradient is weak in SON(0), and tilted in favor of South Atlantic SST anomalies by DJF(1).

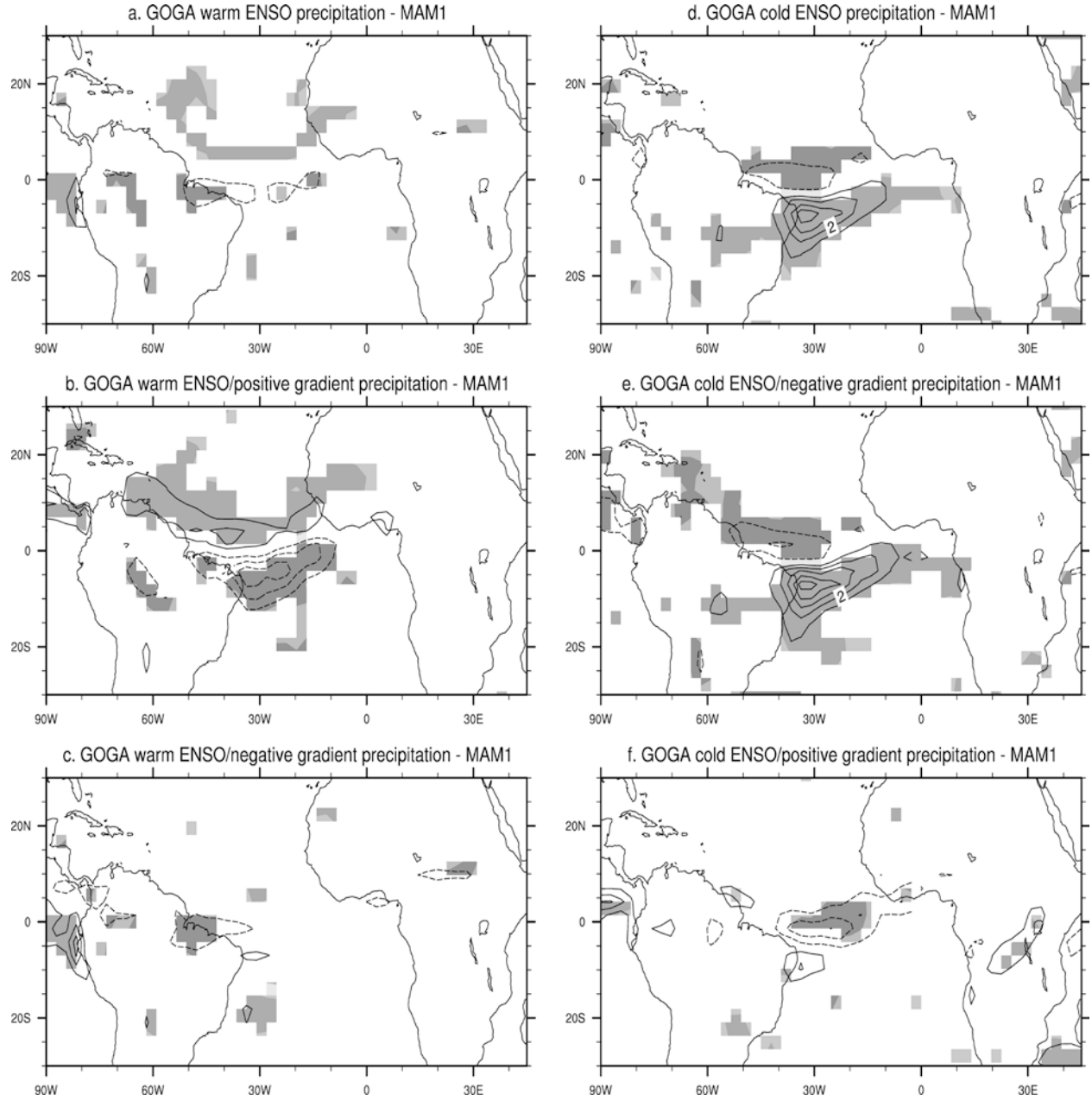

Fig. 6 As in Fig. 3, but for GOGA precipitation. Contour interval is every mm/day

The transition from Southern Hemisphere summer to fall is critical: ENSO and TAV can superimpose or cancel out. If TAV is consistent with the expected, ENSO-related development of tropical North Atlantic SSTs, then the more 'predictable' scenario evolves: ENSO and TAV impacts add up, and strong Nordeste rainfall anomalies develop. If TAV is inconsistent with ENSO, then the less predictable situation of opposing forces is realized. At times, as in 1982–83, ENSO wins out. At other times, as in the more recent 2002–2003 warm event, TAV wins out, tropical South Atlantic SST anomalies persist, and the expected tropical North Atlantic SST and Nordeste rainfall anomalies are not realized. The preconditioning role of the state of the tropical Atlantic on the development of the ENSO teleconnection will be further explored in Sect. 5, using results from the POGAML ensemble. Next we turn to a historical perspective on Nordeste rainfall variability (Sect. 4.2), and to a comparison of the GOGA ensemble of simulations with observations (Sect. 4.3).

4.2 Observed Nordeste rainfall variability (1950–1994)

The distinction between concordant and discordant cases based on the evolution of tropical Atlantic SSTs during an ENSO event is crucial to understanding the asymmetry in observed Nordeste rainfall anomalies, i.e.

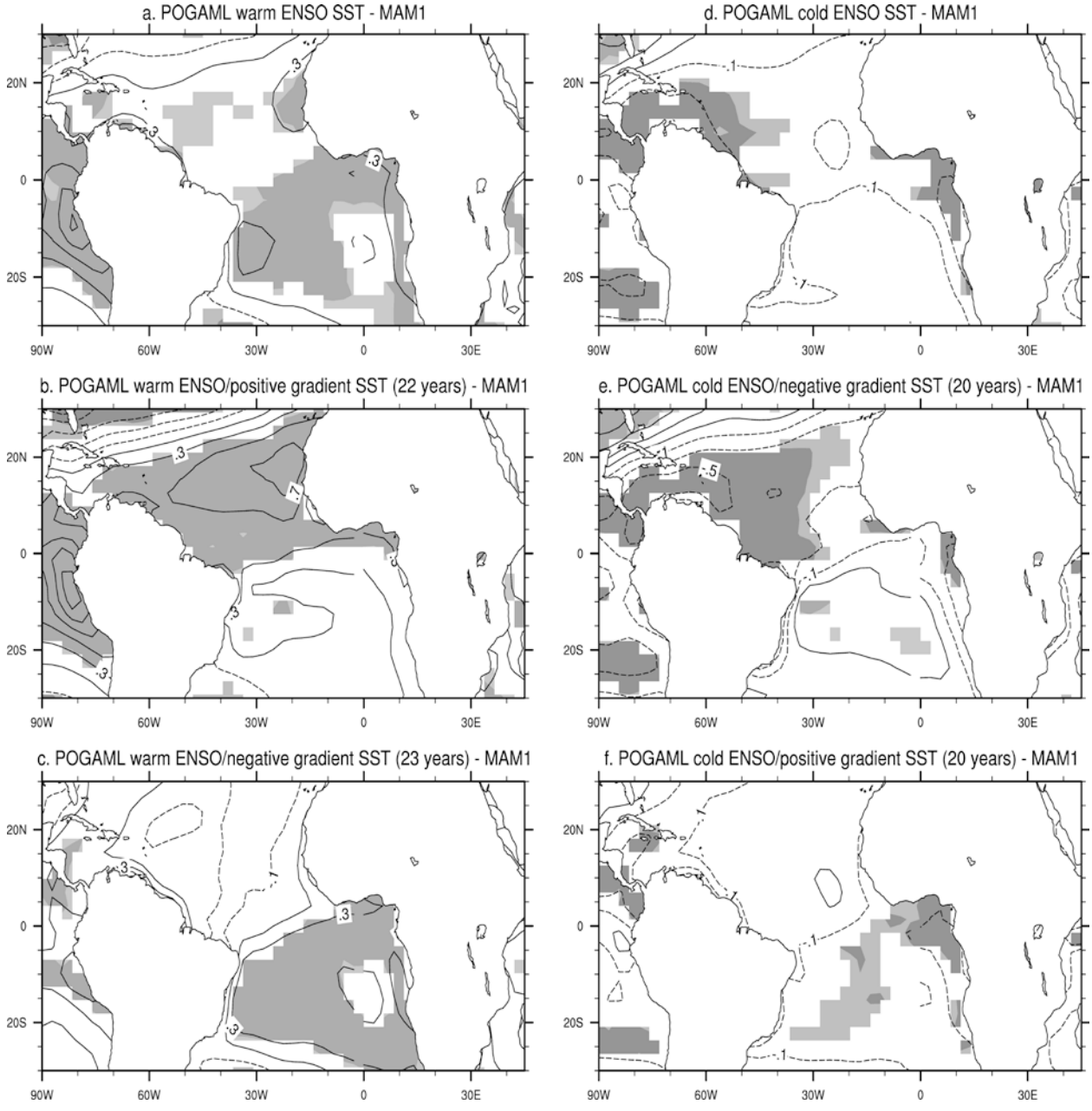

Fig. 7 As in Fig. 3, but for SST simulated in the POGAML ensemble

between the weaker, less significant warm ENSO rainfall anomalies and stronger, statistically significant cold ENSO anomalies (Table 1). Based on the amplitude of tropical Pacific SST anomalies only, which constitute the source perturbation, one would be led to expect the opposite behavior, i.e. that warm ENSO Nordeste anomalies should be larger, consistently with the greater amplitude of tropical Pacific SSTs in warm than in cold events. In fact, only simultaneous consideration of ENSO and TAV can explain this puzzling observation.

The weaker, less statistically significant Nordeste rainfall anomalies in warm than in cold ENSO years during 1950–1994 reflect the weaker, less statistically significant tropical North Atlantic SST anomalies in warm than in cold ENSO events (see top panels of Fig. 3). The latter in turn reflect the greater frequency of discordant cases, i.e. cases in which ENSO and TAV evolve in opposition, in warm than in cold ENSO events. Six out of nine warm ENSO events in 1950–1994 are

►

Fig. 8 The evolution of SST anomalies in warm ENSO concordant (warm ENSO/positive gradient, *left column*) and discordant (warm ENSO/negative gradient, *right column*) cases from the POGAML ensemble, from July–August of year(0) to March–May of year(1). Contour interval is every 0.2 °C starting at 0.1 °C, and *light*/*dark shading* represents the 95/99% level of statistical significance

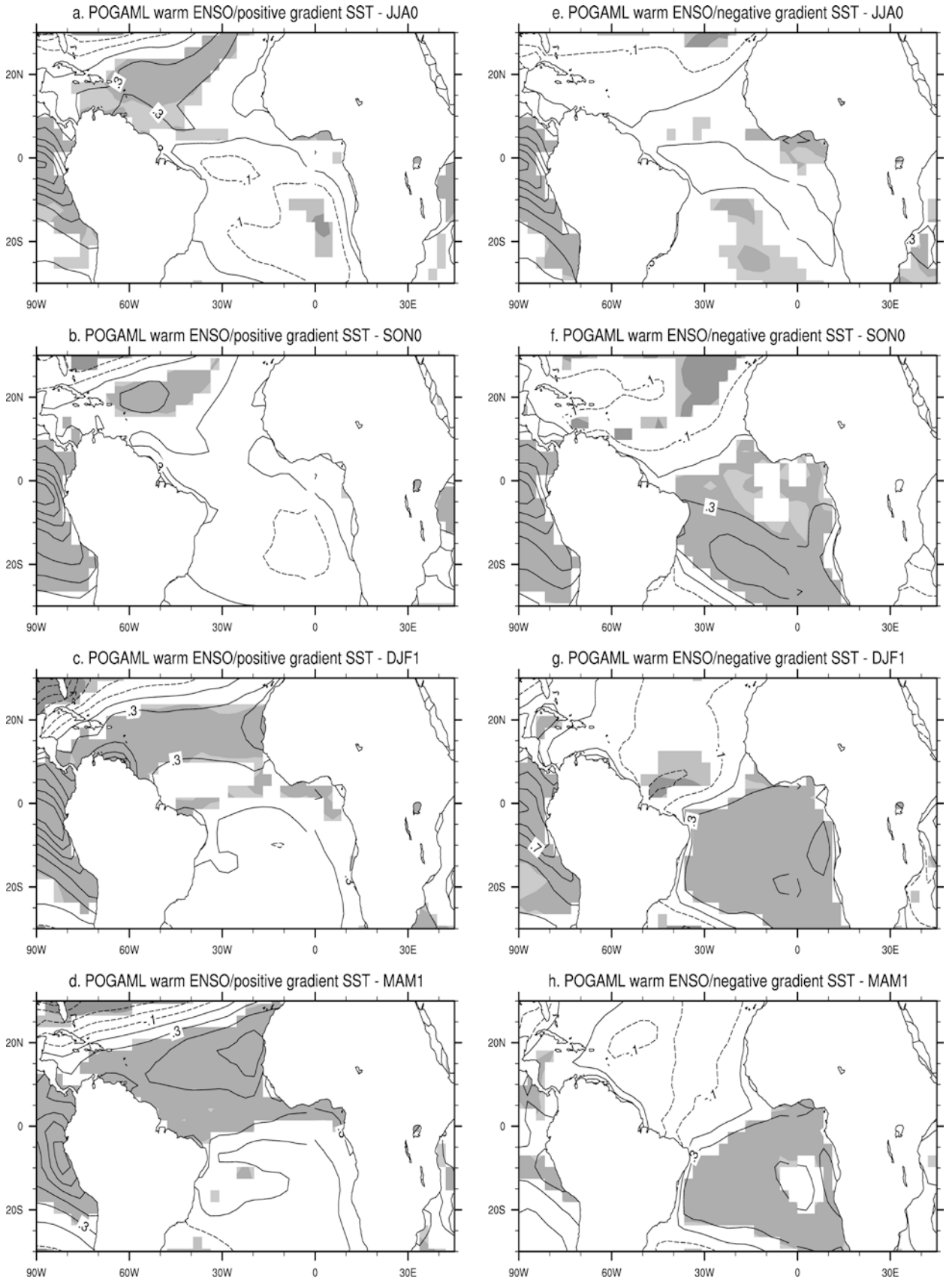
a. POGAML warm ENSO/positive gradient SST - JJA0
e. POGAML warm ENSO/negative gradient SST - JJA0
b. POGAML warm ENSO/positive gradient SST - SON0
f. POGAML warm ENSO/negative gradient SST - SON0
c. POGAML warm ENSO/positive gradient SST - DJF1
g. POGAML warm ENSO/negative gradient SST - DJF1
d. POGAML warm ENSO/positive gradient SST - MAM1
h. POGAML warm ENSO/negative gradient SST - MAM1
20N
0
20S
90W
60W
30W
0
30E

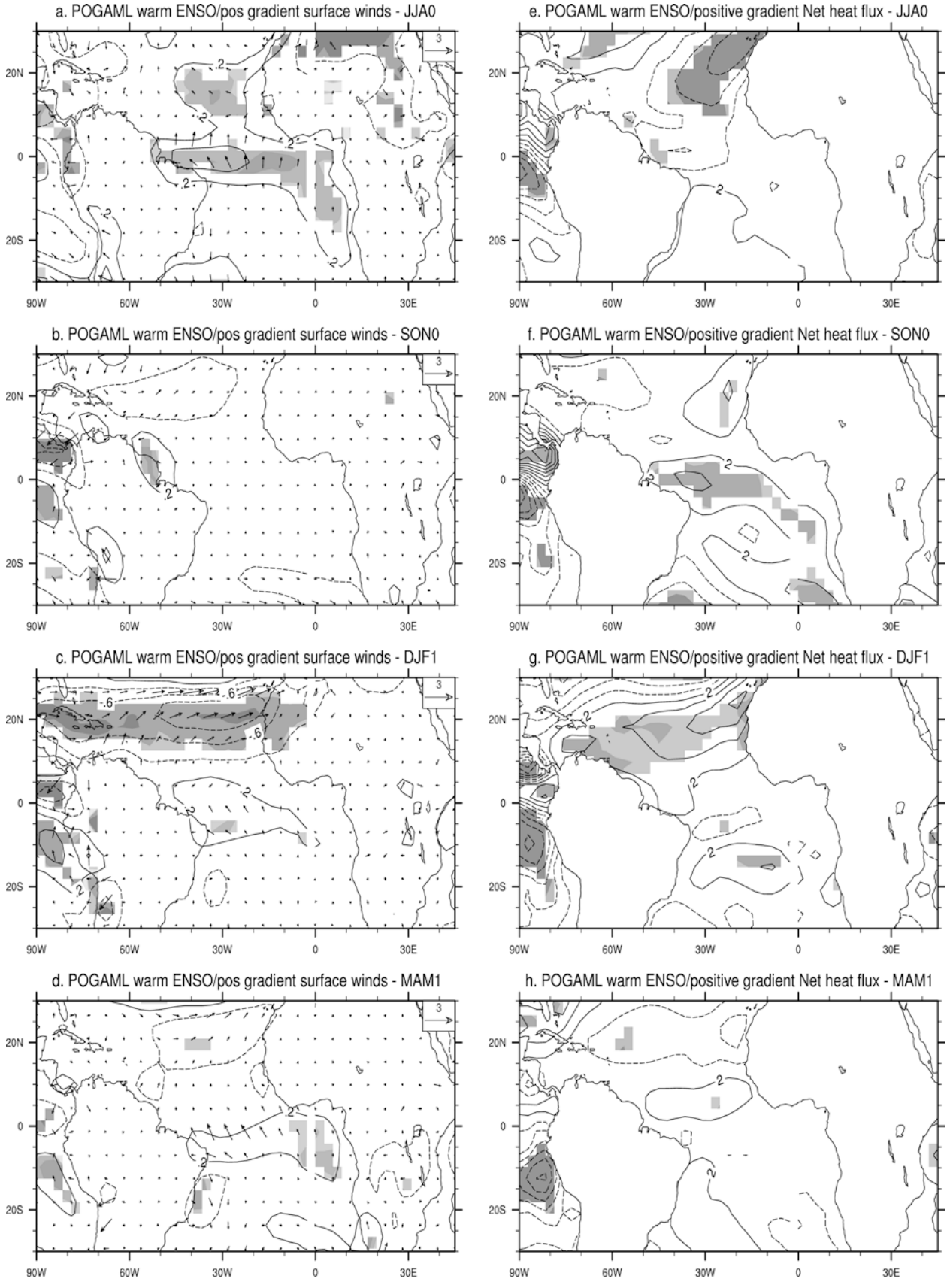
a. POGAML warm ENSO/pos gradient surface winds - JJA0
e. POGAML warm ENSO/positive gradient Net heat flux - JJA0
b. POGAML warm ENSO/pos gradient surface winds - SON0
f. POGAML warm ENSO/positive gradient Net heat flux - SON0
c. POGAML warm ENSO/pos gradient surface winds - DJF1
g. POGAML warm ENSO/positive gradient Net heat flux - DJF1
d. POGAML warm ENSO/pos gradient surface winds - MAM1
h. POGAML warm ENSO/positive gradient Net heat flux - MAM1
20N
0
20S
90W
60W
30W
0
30E

◄

Fig. 9 The evolution of warm ENSO concordant (warm ENSO/positive gradient) anomalies in surface winds (*left column*) and net heat flux (*right column*), positive downward, from the POGAML ensemble, from July–August of year(0) to March–May of year(1). *On the left* contours represent wind speed anomalies, with contour intervals every 0.4 m/s starting at 0.2 m/s, and *light*/*dark shading* represents 95/99% statistical *significance* of the wind speed anomalies. *On the right contour interval* is every 4 W/m^2 starting at 2 W/m^2, and *light*/*dark shading* represents the 95/99% level of statistical significance

discordant, compared to six out of eight cold ENSO events being concordant. The averaging of the stronger, but less frequent warm ENSO/positive gradient cases with the weaker, less coherent, but more frequent warm ENSO/negative gradient cases results in reduced overall significance of the SST and precipitation anomalies. In cold ENSO events, on the other hand, the strong, negative tropical North Atlantic SST anomalies of the concordant cases dominate the picture. Note how in concordant cases the average of Nordeste rainfall anomalies is statistically significant in both warm and cold ENSO events. Conversely, in discordant cases, anomalies are so uncertain that their sign cannot be consistently predicted.

4.3 Validation of Nordeste rainfall variability in the GOGA ensemble

The observed behavior of interannual variability of Nordeste rainfall just described is mirrored in the GOGA ensemble. Model output adds spatial information (Fig. 6) to the observed, regionally-averaged statistics (Table 1). As in observations, rainfall anomalies over the Nordeste, which in the model extend into the western equatorial Atlantic, are weaker in warm than in cold ENSO events. The pattern of all warm ENSO years is more equatorially symmetric compared to the pattern of all cold ENSO years (top panels of Fig. 6), which is more dipolar, or equatorially antisymmetric. In concordant years (middle panels of Fig. 6) warm and cold ENSO patterns are similar, in the dipolar spatial pattern with stronger rainfall anomalies south of the equator, and opposite in sign. Anomalies in discordant years (bottom panels of Fig. 6) are inconsistent, in space and in time.

The asymmetry between weaker Nordeste rainfall anomalies in warm than in cold ENSO events can again be explained by the difference in the frequency of concordant and discordant cases. In the average of warm ENSO events the net effect on the meridional displacement of the Atlantic ITCZ of opposing north and south tropical Atlantic SST anomalies cancels out, leaving exposed the direct, or atmospheric impact of ENSO. This impact is visible in the shape of an equatorially-symmetric Kelvin wave in Fig. 6a. In the mean of cold ENSO events, the more frequent concordant pattern clearly wins out.

5 The POGAML ensemble: potential predictability vof tropical Atlantic SST

In this section, we seek confirmation for the role of the ENSO/TAV interaction in the POGAML ensemble of integrations. This ensemble by construction presents a realistic depiction of tropical ocean-atmosphere interaction where such interaction is dominated by exchanges of energy, not by exchanges of momentum, and is one that can be exploited in dynamical seasonal prediction.

The 5-member POGAML ensemble reproduces reasonably well the ENSO-related SSTs in MAM(1) (compare Fig. 7 with observations in Fig. 3). As in observations, anomalies in concordant/discordant cases occur prevalently in the northern/southern tropics respectively. Warm and cold ENSO events separate according to the sign of the Atlantic SST gradient in equal proportions: 22 concordant versus 23 discordant warm ENSO years, 20 each for concordant and discordant cold ENSO years.

The evolution of SST, surface wind and net heat flux anomalies is depicted in Figs. 8, 9, and 10, for concordant and discordant warm ENSOs only, for the sake of brevity. The differences in the evolution of Atlantic SSTs in concordant and discordant cases are already evident in austral winter of year(0), i.e. June–August, or JJA(0). In the discordant, or warm ENSO/negative gradient case (right column of Fig. 8and Fig. 10) the strongest wind anomalies occur in Southern Hemisphere winter/spring. For instance, a weakened southeasterly flow in the southern sub-tropics is associated with a net heat flux anomaly into the ocean (positive downward) and a co-located positive SST anomaly, around 20°S, 20°W (Fig. 8e,f, and Fig. 10a,b and e,f). The role of internal atmospheric variability during Southern Hemisphere winter in generating these anomalies is currently being investigated (Barreiro et al. submitted 2004). In the warm ENSO/positive gradient case (left column of Fig. 8, Fig. 9) while the local response to a warm north tropical Atlantic SST anomaly is noticed as early as austral winter and spring, the strongest (ENSO-related) surface wind anomalies do not occur until DJF(1) (Fig. 8c,d, and Fig. 9c,g). Then westerly wind anomalies in excess of 1 m/s across the tropical North Atlantic generate large net heat flux anomalies, of the order of 10 W/m^2, and allow SST anomalies of the order of 0.4 °C to grow (Fig. 8c,d).

In DJF(1) and MAM(1), cross-equatorial surface wind anomalies in the warm ENSO/negative gradient case (Fig. 10c,d) are directed towards the tropical South Atlantic SST anomaly. In the warm ENSO/positive gradient case (Fig. 9c,d) they are northward, as expected from the response of TAV to the ENSO-related tropical North Atlantic SST anomalies. The differences in SST, surface winds and precipitation peak in MAM(1) (compare d–h in Figs. 8–10, and b, c in Fig. 3): as the ENSO-related atmospheric bridge enters its decay phase the cross-equatorial flow characteristic of TAV becomes

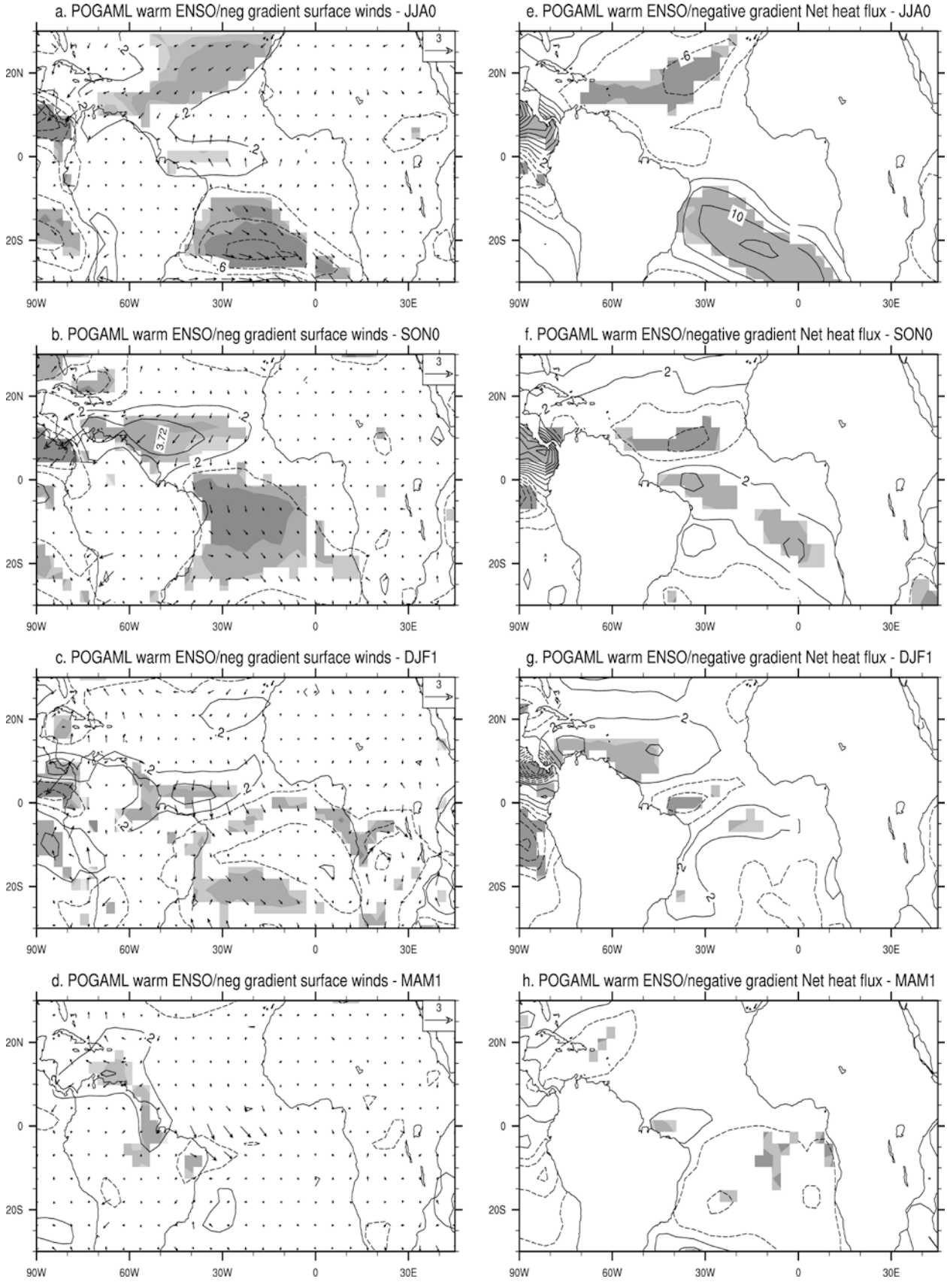

Fig. 10 Same as in Fig. 9, but for warm ENSO discordant (warm ENSO/negative gradient) cases

most evident, and of opposite sign in concordant and discordant composites.

In summary, the observation made on the GOGA ensembles that the development of the 'canonical' response to ENSO in tropical North Atlantic SSTs is strongly dependent on the state of the tropical Atlantic itself is confirmed by the POGAML ensemble. Though the oceanic component of this ocean-atmosphere system is admittedly a very primitive one, the advantage of the POGAML configuration, over GOGA, is that anomalies in this system evolve consistently with each other. Pre-existing SST anomalies are found to condition the development of ENSO-related tropical North Atlantic SST anomalies. When such pre-existing anomalies contrast with the evolution of the ENSO-related tropical North Atlantic SST anomalies, they are able to force an interhemispheric response that greatly hinders the development of the tropical North Atlantic anomalies, limiting them to the far western side of the basin. In both GOGA and POGAML, the presence of warm subtropical South Atlantic SSTs in seasons prior to the mature phase of a warm ENSO was found to be associated with a southward cross-equatorial surface wind flow. Conversely, when pre-existing Atlantic SST anomalies are concordant with the evolution of ENSO-related SSTs, then the two influences, of remote and local SSTs on Nordeste precipitation, add up to give the expected outcome. In either case, the favored pattern in the adjustment of the tropical Atlantic ocean-atmosphere system is meridional in nature, with cross-equatorial surface winds responding and acting upon SST anomalies characterized by a dipolar structure, in a positive wind-evaporation-SST feedback loop (Chang et al. 1997; Xie 1999).

6 Discussion and conclusions

Interannual climate variability in the Brazilian Nordeste has long been the subject of scientific research, due to the intensity of its extremes and the vulnerability of society to them. In recent years the well-documented relation between Nordeste rainfall and sea surface temperatures in the tropical Atlantic and Pacific oceans has fueled interest for the application of seasonal climate prediction (Ward and Folland 1991; Hastenrath 1995) to the management of agricultural and hydrological resources (e.g., De Souza Filho and Lall submitted 2003).

In this study we presented a re-assessment of the Nordeste rainfall-tropical SST relationship that put the spotlight on the interaction between tropical Pacific (El Niño-Southern Oscillation, or ENSO) and Atlantic (Tropical Atlantic Variability, or TAV) patterns of climate variability.

While the role of ENSO in TAV is well known (e.g., Curtis and Hastenrath 1995; Nobre and Shukla 1996; Enfield and Mayer 1997), here we presented evidence to show that the state of the tropical Atlantic as the ENSO event is evolving can precondition the development of the ENSO teleconnection. In years when the interaction between ENSO and TAV leads to a reinforcement of the response, i.e. in the years labelled 'concordant' in this study, the Nordeste rainfall-tropical Atlantic SST relationship was found to be strong, and the amplitude of Nordeste rainfall anomalies larger and more significant than in the complementary 'discordant' years. The latter, which are defined by opposing tendencies in ENSO and TAV with regards to their impact on Nordeste rainfall, were found to be more challenging for prospects of seasonal climate prediction. In 'discordant' years TAV can limit, or even reverse, ENSO's impact on Nordeste rainfall. In seasons leading to the mature phase of ENSO, the persistence of tropical South Atlantic SST anomalies, and of a consistent cross-equatorial response in surface winds, can inhibit the development of the expected tropical North Atlantic SST anomalies. For example, in a warm ENSO event a warm South Atlantic SST anomaly may induce a southward cross-equatorial surface flow that, in feeding back positively on the initial SST anomaly, can preclude the development of a positive SST anomaly in the tropical North Atlantic. Clearly, this is the more 'unstable or unpredictable' case, as its outcome depends on the relative strengths of ENSO and TAV. Barreiro et al. submitted (2004) give a detailed discussion of case studies.

Two possible outcomes of the ENSO teleconnection are outlined:

1. In the absence of significant SST anomalies in the tropical Atlantic, especially in the sub-tropical South Atlantic, during onset and growth phases of ENSO, the ENSO teleconnection follows the expected course: in austral summer and fall anomalies develop in the tropical North Atlantic that are of the same sign as those in the equatorial Pacific. Taken independently, these North Atlantic SST anomalies and the ENSO-related atmospheric anomalies would force Nordeste rainfall anomalies of the same sign. Their concerted effect is coherent Nordeste rainfall anomalies, of negative sign when ENSO is in its warm phase and the tropical North Atlantic warms, of positive sign when ENSO is in its cold phase and the tropical North Atlantic cools.
2. In the presence, in seasons prior to the peak phase of ENSO, of tropical Atlantic SST anomalies configured to induce a meridional gradient opposite in sign to that expected from the growth of the ENSO-related North Atlantic SST anomalies, the coherent response of surface wind and SST to this gradient hinders the full development of the ENSO teleconnection. The response in Nordeste rainfall is more unpredictable, relative to the complementary case, and potentially weakened by the opposition of local and remote forcings.

To what extent sub-tropical South Atlantic SST anomalies themselves are related to ENSO, via a Pacific-South American teleconnection pattern (Mo and Higgins 1998; Cazes-Boezio et al. 2003), or whether

they are more generally the result of internal variability of the Southern Hemisphere winter atmosphere remains to be seen. Certainly their development in seasons prior to mature ENSO conditions in six out of nine warm ENSO events and in two out of eight cold ENSO events over 1950–1994 can explain the observed warm/cold ENSO asymmetry in the strength of the ENSO-Nordeste relationship. In light of the lead time with which they appear, i.e. one to two seasons prior to the Nordeste rainy season, their continued monitoring should lead to an improvement in seasonal climate prediction capabilities.

Acknowledgements We thank Dr. Link Ji for assistance with the integration of CCM3. AG was supported by an NCAR Advanced Study Program Post-doctoral Fellowship, by NASA's Seasonal to Interannual Prediction Project through Interagency Agreement W-19,750 and by NOAA through Grant NA16GP1575. PC was supported by NOAA and NSF through research grants NA16GP1572, ATM-99007625 and ATM-0337846. PC also acknowledges the support from the National Natural Science Foundation of China (NSFC) through Grant 40128003. AG would like to thank Clara Deser for many fruitful discussions and for her continued encouragement. The National Center for Atmospheric Research is operated by the University Corporation for Atmospheric Research under sponsorship of the National Science Foundation.

References

Alexander MA, Bladé I, Newman M, Lanzante JR, Lau N-C, Scott JD (2002) The atmospheric bridge: the influence of ENSO teleconnections on air-sea interaction over the global oceans. J Clim 15: 2205–2231

Biasutti M (2000) Low-frequency variability in the Tropical Atlantic as simulated by the NCAR Climate System Model and the CCM3 coupled to a slab ocean model. 43 pp. Master's Thesis, University of Washington, USA

Cayan DR (1992) Latent and sensible heat flux anomalies over the northern oceans: the connection to monthly atmospheric circulation. J Clim 5: 354–369

Cazes-Boezio G, Robertson AW, Mechoso CR (2003) Seasonal dependence of ENSO teleconnections over South America and relationships with precipitation in Uruguay. J Clim 16: 1159–1176

Chang P, Ji L, Li H (1997) A decadal climate variation in the tropical Atlantic Ocean from thermodynamic air-sea interactions. Nature 385: 516–518

Chang P, Saravanan R, Ji L (2003) Tropical Atlantic seasonal predictability: the roles of El Niño remote influence and thermodynamic air-sea feedback. Geophys Res Lett 30: 1501–1504

Chiang JCH, Kushnir Y, Giannini A (2002) Deconstructing Atlantic ITCZ vasriability: influence of the local cross-equatorial SST gradient, and remote forcing from the eastern equatorial Pacific. J Geophys Res-Atmospheres 107(D1):10.1029/2000JD000307

Chiang JCH, Kushnir Y, Zebiak SE (2000) Interdecadal changes in eastern Pacific ITCZ variability and its influence on the Atlantic ITCZ. Geophys Res Lett 27: 3687–3690

Curtis S, Hastenrath S (1995) Forcing of anomalous sea surface temperature evolution in the tropical Atlantic during Pacific warm events. J Geophys Res 100: 15,835–15,847

Czaja A, van der Vaart P, Marshall J (2002) A diagnostic study of the role of remote forcing in tropical Atlantic variability. J Clim 15: 3280–3290

Easterling DR, Peterson TC, Karl TR (1996) On the development and use of homogenized climate data sets. J Clim 9: 1429–1434

Enfield DB, Mayer DA (1997) Tropical Atlantic sea surface temperature variability and its relation to El Niño-Southern Oscillation. J Geophys Res 102: 929–945

Fisher RA (1970) Statistical methods for research workers, 14th edn. Hafner, New York City, USA, pp 362

Giannini A, Cane MA, Kushnir Y (2001a) Interdecadal changes in the ENSO teleconnection to the Caribbean region and the North Atlantic Oscillation. J Clim 14: 2867–2879

Giannini A, Chiang JCH, Cane MA, Kushnir Y, Seager R (2001b) The ENSO teleconnection to the tropical Atlantic Ocean: contributions of the remote and local SSTs to rainfall variability in the tropical Americas. J Clim 14: 4530–4544

Giannini A, Kushnir Y, Cane MA (2000) Interannual variability of Caribbean rainfall, ENSO and the Atlantic Ocean. J Clim 13: 297–311

Hastenrath S (1991) Climate dynamics of the tropics. Kluwer Academic Dordrecht, The Netherlands

Hastenrath S (1995) Recent advances in tropical climate prediction. J Clim 8: 1519–1532

Hastenrath S, Greischar L (1993) Circulation mechanisms related to northeast Brazil rainfall anomalies. J Geophys Res 98: 5093–5102

Hastenrath S, Heller L (1977) Dynamics of climatic hazards in northeast Brazil QJR Meteorol Soc 103: 77–92

Harzallah A, Aragão JOR, Sadourny R (1996) Interannual rainfall variability in northeast Brazil: observation and model simulation. J Clim 16: 861–878

Kaplan A, Cane MA, Kushnir Y, Clement AC, Blumenthal MB, Rajagopalan B (1998) Analyses of global sea surface temperature 1856–1991. J Geophys Res 103: 18,567–18,589

Kiehl JT, Hack JJ, Bonan GB, Boville BA, Briegleb BP, Williamson DL, Rasch PJ (1996) Description of the NCAR Community Climate Model CCM3. NCAR Technical Note TN-420. NCAR, PO Box 3000, Boulder CO 80307-3000, USA

Kiehl JT, Hack JJ, Bonan GB, Boville BA, Williamson DL, Rasch PJ (1998) The National Center for Atmospheric Research Community Climate Model: CCM3. J Clim 11: 1131–1149

Kiladis GN, Diaz HF (1989) Global climatic anomalies associated with extremes in the Southern Oscillation. J Clim 2: 1069–1090

Koster RD, Suarez MJ, Heiser (2000) Variance and predictability of precipitation at seasonal-to-interannual timescales. J Hydrometeorol 1: 26–46

Kushnir Y, Seager R, Chiang JCH, Miller Velez J (2002) A simple coupled model of tropical Atlantic climate variability. Geophys Res Lett 29: 2133–2136

Lau N-C (1997) Interactions between global SST anomalies and the midlatitude atmospheric circulation. Bull Am Meteorol Soc 78: 21–33

Lau N-C, Nath MJ (1994) A modeling study of the relative roles of tropical and extratropical SST anomalies in the variability of the global atmosphere-ocean system. J Clim 7: 1184–1207

Lau N-C, Nath MJ (1996) The role of the 'atmospheric bridge' in linking tropical Pacific ENSO events to extratropical SST anomalies. J Clim 9: 2036–2057

Levitus S, Boyer T (1994) World Ocean Atlas 1994 vol 4: temperature. NOAA Atlas NESDIS. US Department of Commerce, Washington, DC, USA

Lindzen RS, Nigam S (1987) On the role of sea surface temperature gradients in forcing low-level winds and convergence in the tropics. J Atmos Sci 44: 2418–2436

Magalhaes AR (1993) Drought and policy resposes in the Brazilian northeast In: Wilhite DA (ed) Drought assessment, management, and planning: theory and case studies. Kluwer Academic, Dordrecht, The Netherlands pp 181–189

Mo KC, Higgins RW (1998) The Pacific-South American modes and tropical convection during the Southern Hemisphere winter. Mon Weather Rev 126: 1581–1596

Moron V, Navarra A, Ward MN, Roeckner E (1998) Skill and reproducibility of seasonal rainfall patterns in the tropics in ECHAM-4 GCM simulations with prescribed SST. Clim Dyn 4(2): 83–100

Moura AD, Shukla J (1981) On the dynamics of droughts in northeast Brazil: observations, theory and numerical experi-

ments with a general circulation model. J Atmos Sci 38: 2653–2675
Nobre P, Shukla J (1996) Variations of sea surface temperature, wind stress, and rainfall over the tropical Atlantic and South America. J Clim 9: 2464–2479
Palmer TN, Brankovic C, Viterbo P, Miller MJ (1992) Modeling interannual variations of summer monsoons. J Clim 5: 399–417
Peterson TC, Easterling DR (1994) Creation of homogeneous composite climatological reference series. Int J Climatol 14: 671–679
Pezzi LP, Cavalcanti IFA (2001) The relative importance of ENSO and tropical Atlantic sea surface temperature anomalies for seasonal precipitation over South America: a numerical study. Clim Dyn 17: 205–212
Rasmusson EM, Carpenter TH (1982) Variations in tropical sea surface temperature and surface wind fields associated with the Southern Oscillation/El Niño. Mon Weather Rev 110: 354–384
Reynolds RW, Smith TM (1994) Improved global sea surface temperature analyses using optimum interpolation. J Clim 7: 929–948
Ropelewski CF, Halpert MS (1987) Global and regional precipitation patterns associated with the E1 Niño/Southern Oscillation. Mon Weather Rev 115: 1606–1626
Ropelewski CF, Halpert MS (1996) Quantifying Southern Oscillation-precipitation relationships. J Clim 9: 1043–1059
Saravanan R, Chang P (2000) Interaction between tropical Atlantic variability and E1 Niño-Southern Oscillation. J Clim 13: 2177–2194
Seager R, Kushnir Y, Naik N, Miller J, Chang P, Hazeleger W (2001) Looking for the role of the ocean in tropical Atlantic decadal climate variability. J Clim 14: 638–655
Seager R, Kushnir Y, Visbeck M, Naik N, Miller J, Krahmann G, Cullen H (2000) Causes of Atlantic Ocean climate variability between 1958 and 1998. J Clim 13: 2845–2862
Servain J (1991) Simple climatic indices for the tropical Atlantic Ocean and some applications. J Geophys Res 96: 15,137–15,146
Sperber KR, Palmer TN (1996) Interannual tropical rainfall variability in general circulation model simulations associated with the Atmospheric Model Intercomparison Project. J Clim 9: 2727–2750
Uvo CB, Repelli CA, Zebiak SE, Kushnir Y (1998) The relationships between tropical Pacific and Atlantic SST and Northeast Brazil monthly precipitation. J Clim 11: 551–561
von Storch H, Zwiers FW (1999) statistical analysis in climate research, Cambridge University Press, Cambridge, UK, pp 484
Vose RS, Schmoyer RL, Steurer PM, Peterson TC, Heim R, Karl TR, Eischeid J (1992) The Global Historical Climatology Network: long-term monthly temperature, precipitation, sea level pressure, and station pressure data. ORNL/CDIAC-53, NDP-041. Carbon Dioxide Information Analysis Center, Oak Ridge National Laboratory, Oak Ridge, Tennessee, USA pp 300
Wallace JM, Rasmusson EM, Mitchell TP, Kousky VE, Sarachik ES, von Storch H (1998) On the structure and evolution of ENSO-related climate variability in the tropical Pacific: lessons from TOGA. J Geophys Res 103(C7): 14,241–14,259
Ward MN, Folland CK (1991) Prediction of seasonal rainfall in the north Nordeste of Brazil using eigenvectors of sea surface temperature. Int J Climatol 11: 711–743
Xie S-P (1999) A dynamic ocean-atmosphere model of the tropical Atlantic decadal variability. J Clim 12: 64–70